Fluid mobility in reservoir rocks from integrated VSP and openhole data

Alimzhan Zhubayev (TU Delft), Yang Jihai (CNOOC Ltd.), Cai Jun (CNOOC Ltd.), Igor Borodin (Schlumberger), Michael Sanders (Schlumberger), Teck Kean Lim (Schlumberger), Henry Menkiti (Schlumberger), and Ranajit Ghose (TU Delft)*

SUMMARY

In this study, we first estimate seismic velocity and attenuation dispersion from a comprehensive zero-offset vertical seismic profile (VSP) data acquired in China. These results, combined with openhole data acquired at the same location, provide experimental evidence that the seismic attenuation in rocks is dominated by a fluid-flow mechanism. The loss mechanism due to multiple scattering is found to be negligible. This implies that extraction of fluid mobility (permeability to viscosity ratio) in reservoir rocks using low frequency (10 to 150 Hz) seismic data should be possible. We present a methodology, based on poroelastic inversion using a rotated coordinate system and simulated annealing, to extract fluid mobility from combined VSP and openhole data. Finally, we compare layer-specific fluid mobility values, obtained using this approach, with independent fluid mobility measurements and estimates based on wireline openhole data.

INTRODUCTION

Previous theoretical and experimental studies (e.g., Winkler et al., 1979; Winkler and Nur, 1979; Winkler and Nur, 1982; Akbar et al., 1993; Batzle et al., 2006; Adam et al., 2009) revealed a very strong sensitivity of the seismic waves to pore fluid properties in reservoir rocks. All of these papers conclude that seismic data have a great potential in determining these key physical parameters. Recent rock physics models and advances in field data acquisition help to make this task possible. Particularly, the VSP geometry provides the high-quality seismic data required to address the problem.

To find a direct link between seismic measurements and reservoir properties, Biot proposed the theory of wave propagation in fluid-saturated porous media (Biot, 1962). It models the interaction between the fluid and the solid (porous frame) phases while an elastic waves propagate through a fluid-saturated porous material at a macroscopic scale. This interaction causes the energy of the seismic wave to dissipate due to the viscous flow. However, Biot's theory failed to explain the observed seismic attenuation (see e.g., Dvorkin and Nur, 1993; Dvorkin et al., 1994; Pride et al., 2004), and this led to the development of new poroelastic models.

Different theoretical quantifications of seismic wave attenuation have been proposed in the past (e.g., Dvorkin and Nur, 1993; Dvorkin et al., 1994; Smeulders and van Dongen, 1997; Pride and Berryman, 2003a; Pride and Berryman, 2003b; Muller and Gurevich, 2005). Importantly, it was found that attenuation can peak at seismic frequencies due to a diffusive process (pore-fluid pressure equilibration) at mesoscopic and microscopic (grain) scales. This may occur due to the heterogeneous nature of the solid and the fluid phases. As a result, strong attenuation and velocity dispersion at seismic frequencies can be observed.

In the present research, we start our analysis with the so-called Biot and squirt-flow (BISQ) model (Dvorkin and Nur, 1993). This model has been extensively studied (e.g., Dvorkin et al., 1994; Marketos and Best, 2010) and it has been found to explain well the attenuation and velocity dispersion in typical reservoir rocks. Another advantage of the BISQ model is that it requires less input parameters than the models mentioned previously. This makes the BISQ model more attractive for reservoir characterization. Next, we estimate the attenuation and velocity dispersion from the zero-offset VSP data acquired in China. These results, combined with openhole data, are used in the inversion to obtain fluid mobility in the rock formation. In the inversion, we minimize the objective function using a rotated coordinate system and simulated annealing (Collins and Fishman, 1995).

THE BISQ MODEL

The BISQ model unifies two loss mechanisms: 1) the Biot loss mechanism, which accounts for the viscous loss due to fluid flow in the direction of the solid motion (global flow) and 2) the squirt-flow, which occurs when the fluid is squeezed out of the thin cracks to the stiff pores as a seismic wave propagates through a partially (or apparently fully) saturated porous media. The model assumes that the fluid and the solid phases are homogeneous and isotropic. A Newtonian fluid can flow not only parallel, but also perpendicular to the direction of wave propagation. All thermal and chemical effects are ignored. The model derivation can be found in Dvorkin and Nur (1993). Here we show only the final expressions for fast and slow *P*-wave velocities ($V_{P_{1,2}}$) and attenuations ($\alpha_{P_{1,2}}$):

$$V_{P_{1,2}} = \frac{1}{\mathrm{Re}\left(\sqrt{Y_{1,2}}\right)}, \tag{1}$$

$$\alpha_{P_{1,2}} = \omega \mathrm{Im}\left(\sqrt{Y_{1,2}}\right), \text{ where} \tag{2}$$

$$Y_{1,2} = -\frac{B}{2A} \pm \sqrt{\left(\frac{B}{2A}\right)^2 - \frac{C}{A}}, \tag{3}$$

$$A = \frac{F_{sq} M}{n \rho_f^2}, \tag{4}$$

$$B = \frac{F_{sq}\left(2\alpha - n - \frac{(1-n)\rho_s}{\rho_f}\right) - \left(M + F_{sq}\frac{\alpha^2}{n}\right)\left(1 + \frac{\rho_a}{n\rho_f} + i\frac{\omega_c}{\omega}\right)}{n\rho_f}, \tag{5}$$

DOI http://dx.doi.org/10.1190/segam2013-0213.1

$$C = \frac{(1-n)\rho_s}{n\rho_f} + \left(1 + \frac{(1-n)\rho_s}{n\rho_f}\right)\left(\frac{\rho_a}{n\rho_f} + i\frac{\omega_c}{\omega}\right), \quad (6)$$

$$\rho_a = (\gamma - 1)n\rho_f, \quad (7)$$

$$\omega_c = \frac{\mu n}{k\rho_f}, \quad (8)$$

$$\lambda^2 = \frac{\rho_f \omega^2}{F}\left(\frac{n + \frac{\rho_a}{\rho_f}}{n} + i\frac{\omega_c}{\omega}\right), \quad (9)$$

$$F = \left(\frac{1}{K_f} + \frac{1-\alpha}{nK}\right)^{-1}, \text{ and} \quad (10)$$

$$F_{sq} = F\left(1 - \frac{2J_1(\lambda R)}{\lambda R J_0(\lambda R)}\right). \quad (11)$$

Let us now identify the inputs for these equations. $\alpha = 1 - \frac{K}{K_s}$, where K is the bulk modulus of the rock in drained condition, and K_s is the bulk modulus of the solid grain. M is the dry uniaxial modulus, K_f is the fluid bulk modulus, μ is the viscosity of the fluid, k is the permeability, ρ_s is the density of the grain, ρ_f is the density of the fluid, n is the porosity, γ is the tortuosity, ω and ω_c, respectively, are the cyclic and Biot characteristic frequencies, and R is the characteristic squirt-flow length. J_0 and J_1 are the Bessel function of zero and first order, respectively.

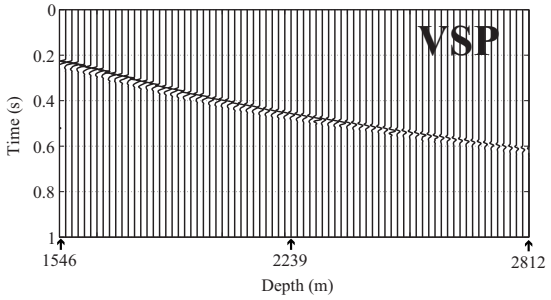

Figure 1: Stacked zero-offset VSP data acquired in China. A time window around the peak amplitude of the direct *P*-wave first arrival is applied.

FIELD ZERO-OFFSET VSP AND OPENHOLE DATA

High-quality zero-offset VSP (Figure 1) and wireline log data (Figure 2) were acquired in China at the same location. The VSP acquisition geometry included seismic sensors positioned in the vertical borehole in turn at 15-m and 30-m intervals. At depths $>$ 2178 m, the sensors were positioned at a 15-m interval. The time sampling is 1 ms. The wireline log data was acquired (and interpreted) every 15 cm, which included bulk density, porosity, Stoneley wave-based mobility and *P*- and *S*-wave velocity measurements. In addition, high-resolution magnetic resonance and dynamic formation test measurements were performed to obtain independent estimates of fluid mobility in the formation. Two independent porosity calculations for the same openhole were available (see Figure 2).

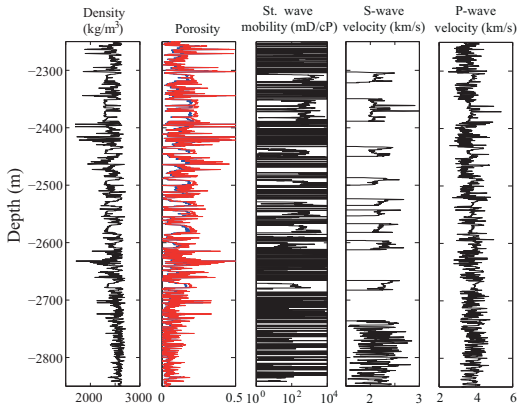

Figure 2: Wireline logs and interpreted data. Logs were acquired in the same well as the VSP data.

ESTIMATION OF ATTENUATION AND VELOCITY DISPERSION FROM VSP DATA

The VSP data (Figure 1) is used to extract layer-specific intrinsic seismic attenuation and velocity dispersion. No processing is applied to the stacked raw seismograms in order to preserve the intrinsic properties of the data. This is critical, especially for the attenuation estimation, where the use of true amplitudes is essential. In order to extract stable dispersion and attenuation information within a given layer, we use the approach of Zhubayev and Ghose (2012b).

Figure 3 shows the results of attenuation and velocity dispersion estimates for depth intervals where seismic (VSP) data at four consecutive depth were available. In other words, four traces are used within each sliding window, with a step of one trace, to calculate layer-specific attenuation and velocity dispersion.

The dispersion analysis reveals a strong correlation between well log data, velocity and attenuation estimates. Strong correlations are marked by the red arrows in Figure 3. One can see relatively conspicuous attenuation and velocity dispersion for sandy zones in which the hydrocarbons are accumulated. Further, the results clearly indicate that the attenuation is more sensitive to the fluid content of the formation than to seismic velocity. Distinct signatures of mobility changes on seismic amplitudes are delineated. These results can be regarded as field evidences of wave-induced fluid flow in the reservoir rock causing seismic wave attenuation.

The observed effective attenuation is the sum of intrinsic and scattering attenuations. Analysis of the relative impact of geometrical spreading, inelastic absorption, and scattering attenuation on the effective attenuation is necessary. Previous studies (O'Doherty and Anstey, 1971; Schoenberger and Levin, 1974) suggest that, in the scale of seismic wavelengths, the primary extrinsic loss may be caused by the multiple layering. To quantify the scattering attenuation attributed to the multiple layering, we use the deterministic technique proposed by Wapenaar et al. (2003).

DOI http://dx.doi.org/10.1190/segam2013-0213.1

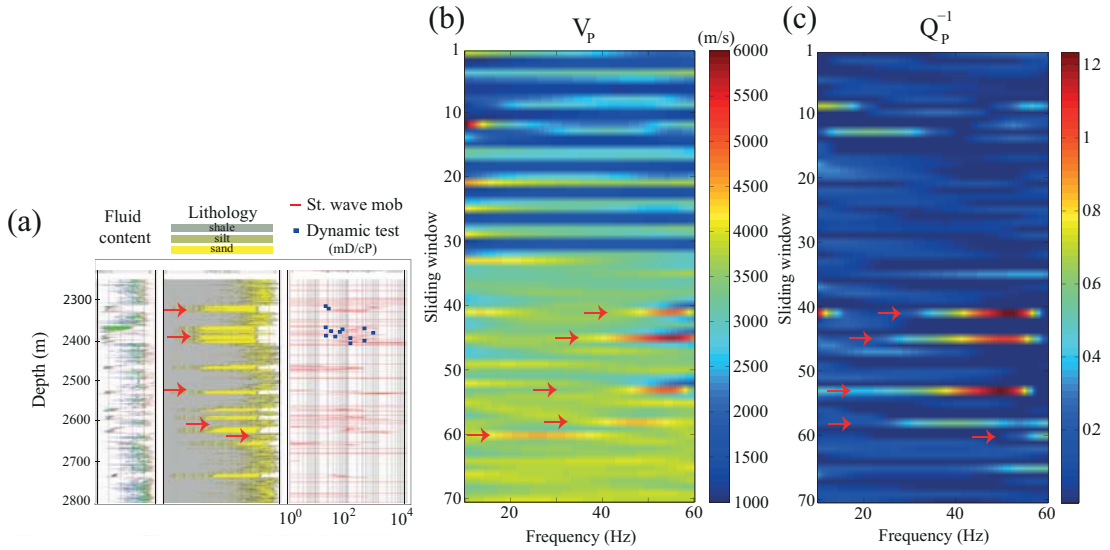

Figure 3: Vertical profiles showing fluid content (green color is oil), lithology and mobility of the formation (a); and estimated interval velocity (b) and attenuation dispersion (c) between 1546 and 2812 m depth.

To calculate scattering attenuation (Q_{sc}^{-1}), *P*-wave velocity and density logs were utilized. We found that the scattering attenuation (Q_{sc}^{-1}) to be < 0.01 for frequencies below 150 Hz. Further comparison with the apparent attenuation estimated from the VSP data (see Figure 3c) suggests that the contribution of the scattering attenuation to the apparent attenuation is negligible. Thus, scattering attenuation alone cannot predict the relatively high attenuation for almost all depth zones, and even more so for attenuation values observed in sandy zones. It appears that the observed attenuation of seismic waves is primarily due to intrinsic loss due to fluid flow, especially in sandy zones. Thus, extraction of transport properties from seismic data should be feasible.

POROELASTIC INVERSION USING A ROTATED COORDINATE SYSTEM AND SIMULATED ANNEALING

Combined use of dispersive seismic velocity and attenuation in a cost function can be advantageous (Zhubayev and Ghose, 2012a). Thus, we use dispersive fast *P*-wave velocity $V_P(\omega,\vec{x})$ and attenuation $\alpha_P(\omega,\vec{x})$ in an integrated cost function:

$$C_{V,\alpha} = \left(W_1 \sum_{\omega} \left| \Delta_P^V \right|^{\beta} + W_2 \sum_{\omega} |\Delta_P^{\alpha}|^{\beta} \right)^{\frac{1}{\beta}}, \qquad (12)$$

where $\Delta_P^V = \frac{V_P(\omega,\vec{x}) - \widehat{V_P}(\omega)}{\sigma_V(\omega)}$, $V_P(\omega,\vec{x})$ being the velocity estimated from a pertinent model of poroelasticity and $\widehat{V_P}(\omega)$ representing intrinsic velocity dispersion extracted from the field data. The term $\vec{x}$ is the model input parameter vector, and $\sigma_V(\omega)$ denotes the standard deviation in the velocity estimate. For the attenuation, the notations for Δ_P^{α} are similar, and W_1 and W_2 are appropriate scaling coefficients, which can be calculated prior to the inversion.

We use a simulated annealing optimization algorithm (Kirkpatrick et al., 1983; Metropolis et al., 1953) to minimize Eq. 12 and, in this way, to obtain the BISQ parameters. The optimization efficiency can be improved by navigating this global search algorithm using a rotated coordinates method (Collins and Fishman, 1995). We compute rotated coordinates to obtain more information on how the parameters are coupled to each other and to determine the relative sensitivity of the velocity and attenuation dispersion to changes in the model parameters. This can be obtained by calculating the eigenvector and the eigenvalues of the covariance matrix of the cost function gradient (Collins and Fishman, 1995):

$$\Psi = \int_{\Omega} \nabla C_{V,\alpha} (\nabla C_{V,\alpha})^t d\Omega, \qquad (13)$$

where Ω is the parameter space.

$$\Omega = \{\vec{x} | a_i < x_i < b_i\}, \qquad (14)$$

where a_i and b_i are the bounds on the ith parameter. Parameter vector $\vec{x}$ contains the parameters x_i for $i = \overline{1,N}$. In order to meaningfully compare the elements in $\vec{x}$, the dimensions are removed by dividing x_i by $b_i - a_i$. Monte Carlo integration is used to efficiently calculate the multidimensional integral (Eq. 13).

The parameter search space Ω (or parameter bounds) can be identified on the basis of exhaustive openhole data which were available. The BISQ model requires twelve parameters. Ten parameters from the BISQ model can be extracted with relative success from the well log data. However, the other two rock properties—tortuosity (γ) and characteristic squirt length (R)—are difficult or virtually impossible to measure. Stoll (1977)

DOI http://dx.doi.org/10.1190/segam2013-0213.1

shows that the tortuosity may range from 1 to 3. On the other hand, from eigenvector analysis of the covariance matrix (Ψ), the sensitivity of tortuosity to velocity and attenuation dispersion is found to be rather small. This is because we are at much lower frequencies compared to the Biot's characteristic frequency. Information concerning the characteristic squirt length is not known and can only be obtained by fitting the BISQ model to the observed velocity dispersion and attenuation. A broad range for the squirt-flow length is, therefore, chosen (0.001 to 100 mm). The squirt-flow length for reservoir sandstones was rigorously studied by Marketos and Best (2010). Realistic bounds for the fluid properties such as viscosity, density, and bulk modulus, are approximately defined from the fluid content information and are checked with the values calculated from the thermodynamic relationships and empirical trends (Batzle and Wang, 1992). The shear rigidity bounds are approximately calculated from the velocity-rigidity-density relationship ($G = \rho V_S^2$). The bounds for the frame bulk modulus are calculated using Gassmann's equation. Typical grain density and grain bulk modulus ranges are taken. Poisson's ratio is calculated from the V_P/V_S ratio.

The inversion scheme is accomplished at each depth zone (see Figure 3), minimizing the cost function $C_{V,\alpha}$ in Eq. 12. Layer-specific output parameters are obtained for 40 realizations of simulated annealing at each depth interval. Median values are then calculated from the 40 vector outputs for a given layer. The results of the median layer-specific mobility inverted from the VSP and openhole data are shown in Figure 4c. We can see a fairly good correlation between the Stoneley wave-based mobility, formation test mobility, and fluid mobility obtained from this study.

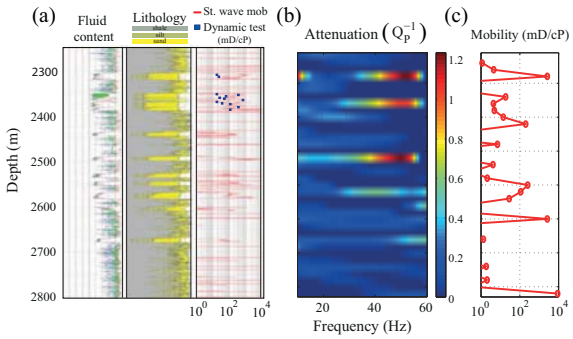

Figure 4: Vertical well profiles showing fluid content, lithology and fluid mobility (a); estimated interval attenuation from the VSP data (b); and (c) inverted interval mobility values using the approach proposed in this work.

Although the scale of the inverted fluid mobilities are different between the Stoneley wave-based and formation test mobilities, one can see that the absolute magnitude of the mobility estimates extracted in this study are comparable at several depth intervals. The goodness of the mobility estimates and the model can also be checked by fitting the observed data with the BISQ model. One of these tests is illustrated in Figure 5. The BISQ model fits the data very well, indicating that the squirt-flow might be dominating and responsible for the observed dissipative process at seismic frequencies and can be used in addressing reservoir transport properties.

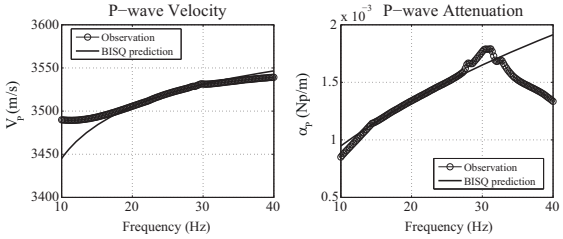

Figure 5: Estimated seismic velocity and attenuation dispersion from the VSP data (2300 to 2405 m depth interval) and compared with BISQ model predictions.

CONCLUSIONS

Our new approach, based on the BISQ model and using VSP and openhole data, provided an in situ estimation of rock transport properties in reservoir rocks. In general, the theoretical prediction from the BISQ model was in a very good agreement with the observed seismic velocity dispersion and attenuation. This indicated that squirt-flow might be a dominant dissipative mechanism and pertinent to the formation under consideration. The relatively strong velocity and attenuation dispersion values observed at sandy zones saturated with fluid was direct evidence supporting the validity of seismic wave attenuation in reservoir rocks due to wave-induced fluid flow. The impact of scattering attenuation on the apparent attenuation was quantified in this study and found to be negligible. Prior to inversion, the relative importance, coupling and sensitivity of the BISQ parameters were studied using eigenvector analysis of the covariance matrix of the gradient of the cost function to efficiently navigate the optimization technique. Finally, a poroelastic inversion using a rotated coordinate system and simulated annealing successfully handled the multiparameter inversion problem. The proposed approach provided stable and reliable fluid mobility values that compared well with the independent Stoneley wave-based and formation test mobilities at the same location. Although the scale of the inverted fluid mobilities was different from the Stoneley wave-based and test data fluid mobilities, the absolute magnitudes and the general trend of the extracted fluid mobilities were comparable.

ACKNOWLEDGMENTS

We thank China National Offshore Oil Corporation (CNOOC) Ltd. for permission to publish these data. The authors thank Samantha Perkins (Schlumberger) and Scott Leaney (Schlumberger) for their valuable comments and suggestions. The research of AZ was supported by Deltares and the Delft Earth research programme of the Delft University of Technology.

DOI http://dx.doi.org/10.1190/segam2013-0213.1

http://dx.doi.org/10.1190/segam2013-0213.1

EDITED REFERENCES

Note: This reference list is a copy-edited version of the reference list submitted by the author. Reference lists for the 2013 SEG Technical Program Expanded Abstracts have been copy edited so that references provided with the online metadata for each paper will achieve a high degree of linking to cited sources that appear on the Web.

REFERENCES

Adam, L., M. Batzle, K. Lewallen, and K. van Wijk, 2009, Seismic wave attenuation in carbonates: Journal of Geophysical Research, **114**, B06208, http://dx.doi.org/10.1029/2008JB005890.

Akbar, N., J. Dvorkin, and A. Nur, 1993, Relating P-wave attenuation to permeability: Geophysics, **58**, 20–29, http://dx.doi.org/10.1190/1.1443348.

Batzle, M., D. Han, and R. Hofmann, 2006, Fluid mobility and frequency-dependent seismic velocity-direct measurements: Geophysics, **71**, no. 1, N1–N9.

Batzle, M., and Z. Wang, 1992, Seismic properties of pore fluids: Geophysics, **57**, 1396–1408, http://dx.doi.org/10.1190/1.1443207.

Biot, M., 1962, Mechanics of deformation and acoustic propagation in porous media: Journal of Applied Physics, **33**, 1482–1498, http://dx.doi.org/10.1063/1.1728759.

Collins, M., and L. Fishman, 1995, Efficient navigation of parameter landscapes: The Journal of the Acoustical Society of America, **98**, 1637–1644, http://dx.doi.org/10.1121/1.413430.

Dvorkin, J., R. Nolen-Hoeksema, and A. Nur, 1994, The squirt-flow mechanism: Macroscopic description: Geophysics, **59**, 428–438, http://dx.doi.org/10.1190/1.1443605.

Dvorkin, J., and A. Nur, 1993, Dynamic poroelasticity: A unified model with the squirt and the Biot mechanisms: Geophysics, **58**, 524–533.

Kirkpatrick, S., C. D. Gelatt, Jr., and M. P. Vecchi, 1983, Optimization by simulated annealing: Science, **220**, 671–680, http://dx.doi.org/10.1126/science.220.4598.671.

Marketos, G., and A. Best, 2010, Application of the BISQ model to clay squirt flow in reservoir sandstones: Journal of Geophysical Research, **115**, B6, B06209, http://dx.doi.org/10.1029/2009JB006495.

Metropolis, E., A. Rosenbluth, M. Rosenbluth, A. Teller, and E. Teller, 1953, Equation of state calculations by fast computing machines: The Journal of Chemical Physics, **21**, 1087–1092, http://dx.doi.org/10.1063/1.1699114.

Müller, T. M., and B. Gurevich, 2005, Wave-induced fluid flow in random porous media: attenuation and dispersion of elastic waves: The Journal of the Acoustical Society of America, **117**, 2732–2741, http://dx.doi.org/10.1121/1.1894792.

O'Doherty, R., and N. Anstey, 1971, Reflections on amplitudes: Geophysical Prospecting, **19**, 430–458, http://dx.doi.org/10.1111/j.1365-2478.1971.tb00610.x.

Pride, S., and J. Berryman, 2003a, Linear dynamics of double-porosity dual-permeability materials I. Governing equations and acoustic attenuation: Physical Review E: Statistical, Nonlinear, and Soft Matter Physics, **68**, 036603, http://dx.doi.org/10.1103/PhysRevE.68.036603.

Pride, S. R., and J. G. Berryman, 2003b, Linear dynamics of double-porosity dual-permeability materials. II. Fluid transport equations: Physical Review E: Statistical, Nonlinear, and Soft Matter Physics, **68**, 036604, http://dx.doi.org/10.1103/PhysRevE.68.036604.

Pride, S., J. Berryman, and J. Harris, 2004, Seismic attenuation due to wave-induced flow: Journal of Geophysical Research, **109**, B01201, http://dx.doi.org/10.1029/2003JB002639.

Schoenberger, M., and F. Levin, 1974, Apparent attenuation due to intrabed multiples: Geophysics, **18**, 10–40.

Smeulders, D., and M. van Dongen, 1997, Wave propagation in porous media containing a dilute gas-liquid mixture: Theory and experiments: Journal of Fluid Mechanics, **343**, 351–373, http://dx.doi.org/10.1017/S0022112097005983.

Stoll, R., 1977, Acoustic waves in ocean sediments: Geophysics, **42**, 715–725, http://dx.doi.org/10.1190/1.1440741.

Wapenaar, C., D. Draganov, and J. Thorbecke, 2003, Relations between codas in reflection and transmission data and their applications in seismic imaging: Presented at the 6th SEGJ International Symposium on Imaging Technology.

Winkler, K., and A. Nur, 1979, Pore fluids and seismic attenuation in rocks: Geophysical Research Letters, **6**, 1–4, http://dx.doi.org/10.1029/GL006i001p00001.

Winkler, K., and A. Nur, 1982, Seismic attenuation: Effects of pore fluids and frictional sliding: Geophysics, **47**, 1–15, http://dx.doi.org/10.1190/1.1441276.

Winkler, K., A. Nur, and M. Gladwin, 1979, Friction and seismic attenuation in rocks: Nature, **277**, 528–531, http://dx.doi.org/10.1038/277528a0.

Zhubayev, A., and R. Ghose, 2012a, Contrasting behavior between dispersive seismic velocity and attenuation: Advantages in subsoil characterization: The Journal of the Acoustical Society of America, **131**, no. 2, EL170–EL176, http://dx.doi.org/10.1121/1.3678692.

Zhubayev, A. and R. Ghose, 2012b, Physics of shear-wave intrinsic dispersion and estimation of in situ soil properties: A synthetic VSP appraisal: Near Surface Geophysics, **10**, 613–629.